AD_____

Award Number: DAMD17-03-1-0257

TITLE: Nanoparticle-mediated Rescue of p53 Through Targeted Degradation of MDM2

PRINCIPAL INVESTIGATOR: Nicholas O. Fischer
Vincent M. Rotello

CONTRACTING ORGANIZATION: University of Massachusetts
Amherst, MA 01003

REPORT DATE: September 2005

TYPE OF REPORT: Annual Summary

PREPARED FOR: U.S. Army Medical Research and Materiel Command
Fort Detrick, Maryland 21702-5012

REPORT DOCUMENTATION PAGE

Form Approved
OMB No. 0704-0188

1. REPORT DATE	2. REPORT TYPE	3. DATES COVERED
01-09-2005	Annual Summary	18 Aug 2004 – 17 Aug 2005

4. TITLE AND SUBTITLE

Nanoparticle-mediated Rescue of p53 Through Targeted Degradation of MDM2

5a. CONTRACT NUMBER

5b. GRANT NUMBER
DAMD17-03-1-0257

5c. PROGRAM ELEMENT NUMBER

6. AUTHOR(S)

Nicholas O. Fischer
Vincent M. Rotello

5d. PROJECT NUMBER

5e. TASK NUMBER

5f. WORK UNIT NUMBER

7. PERFORMING ORGANIZATION NAME(S) AND ADDRESS(ES)

University of Massachusetts
Amherst, MA 01003

8. PERFORMING ORGANIZATION REPORT NUMBER

9. SPONSORING / MONITORING AGENCY NAME(S) AND ADDRESS(ES)
U.S. Army Medical Research and Materiel Command
Fort Detrick, Maryland 21702-5012

10. SPONSOR/MONITOR'S ACRONYM(S)

11. SPONSOR/MONITOR'S REPORT NUMBER(S)

12. DISTRIBUTION / AVAILABILITY STATEMENT
Approved for Public Release; Distribution Unlimited

13. SUPPLEMENTARY NOTES

14. ABSTRACT

The interaction between MDM2 and p53 is a viable therapeutic target, as overexpression of MDM2 can lead to excessive p53 degradation, suppressing a cell's ability to cope with cellular insult. The goal of this research is to use recent advances in nanotechnology to develop a specific nanoparticle antagonist to disrupt the MDM2:p53 interaction. Inhibiting the interaction between p53 and MDM2 allows wild-type p53 concentrations to rise to functional levels, effectively killing proliferating tumor cells. By incorporating traditional peptide inhibitors of MDM2 with mixed-monolayer protected gold cluster nanoparticles, we hope to effect MDM2 denaturation on the nanoparticle surface, increase peptide stability, and facilitate intracellular peptide delivery. Nanoparticle characteristics, such as size, surface chemistry and biocompatibility, may be controlled and modified for these specific applications. Preliminary research demonstrated that nanoparticle-peptide conjugates can indeed inhibit MDM2. In the second year of the research grant, certain aspects of nanoparticle and peptide design were addressed to facilitate purification and quantification of the nanoparticle-peptide conjugates. These studies are necessary to validate the preliminary findings of inhibition.

15. SUBJECT TERMS
MDM2, p53, nanoparticles, peptides

16. SECURITY CLASSIFICATION OF:			17. LIMITATION OF ABSTRACT	18. NUMBER OF PAGES	19a. NAME OF RESPONSIBLE PERSON
a. REPORT	b. ABSTRACT	c. THIS PAGE			USAMRMC
U	U	U	UU	12	19b. TELEPHONE NUMBER *(include area code)*

Table of Contents

Introduction

The interaction between MDM2 and p53 is a viable therapeutic target. Overexpression of MDM2 can lead to excessive degradation of p53, suppressing a cell's ability to cope with cellular insult.[1] MDM2-conferred tumorigenicity has been implicated in a number of human tumors, including breast cancer.[2-5] Disruption of the MDM2:p53 interaction enables functional levels of p53 to accumulate, allowing cells to either halt cell division or initiate apoptosis.[6] Numerous studies have been successful in disrupting the MDM2:p53 interaction using inhibitory peptides,[7,8] peptide analogs,[9-11] or polycyclic compounds.[12-16] These inhibitors target the deep hydrophobic cleft of MDM2 that interacts with the N-terminal α-helix of p53. Although promising, many of these approaches have inherent challenges ranging from stability in cellular environments to cellular delivery. Based on these limitations, an approach integrating specificity, stability, internalization and biocompatibility is needed. The advent of nanoparticle technology may present an ideal way to address these issues.

Our group has demonstrated the versatility of nanoparticles in biological settings, ranging from plasmid transfection of mammalian cells to tunable binding of protein surfaces.[17-20] These studies validate the biological application of nanoparticles and suggest that they can be used to inhibit MDM2. The disruption of the p53:MDM2 interaction can rescue cells that are characterized by wild type p53 and overexpressed MDM2. Nanoparticles functionalized with a previously studied p53 peptide[7] will be used to specifically bind MDM2. Upon binding, MDM2 may denature on the surface of the nanoparticle, removing the potential for release and further action on p53. Given the relative size and surface functionality, each nanoparticle will be able to bind multiple copies of MDM2. This provides an efficient means of effectively decreasing intracellular MDM2 concentrations, allowing p53 to reach wild type levels, thus enabling a cellular approach to tumor elimination.

The first project year successfully addressed: 1) expression and purification of recombinant proteins and ELISA development, 2) synthesis of peptide-tagged nanoparticle, and 3) validation of the proposed hypothesis in an *in vitro* setting.

Body

While preliminary results demonstrate the effective inhibition of the MDM2:p53 interaction by peptide-decorated nanoparticles, an issue of concern was raised over the purity of the nanoparticle-peptide conjugates. The initial method of synthesis made determination of both nanoparticle purity and peptide incorporation difficult. For this reason, it was not possible to conclude with absolute certainty that the inhibition observed was no influenced by the presence of unconjugated peptide remaining in solution. Coupled with inconclusive data on peptide concentrations, these data required verification. To do this, certain issues needed to be addressed: 1) determination of the peptide concentration on the nanoparticle surface to allow direct comparisons of inhibition by NP-peptide and free peptide. 2) adequate nanoparticle purification to avoid erroneous inhibition profiles by unincorporated peptide ligands, and 3) increasing the spacing between peptide and nanoparticle surface to ensure a spatially favorable presentation of the peptide. To address these issues, modifications in the design of the peptide, the thiol linker, and the nanoparticle were required.

Peptide and thiol linker optimization

Peptide solubility is an important factor in nanoparticle purification and accurate determination of peptide concentration. If completely water soluble, the peptide ligand can be separated from the peptide-nanoparticle conjugate by either centrifugation or dialysis, and, by determining peptide concentration in the centrifugation supernatants and washes, the amount of unincorporated can be quantified. This allows an approximate estimation of the degree of peptide incorporation into the nanoparticle monolayer. Peptide 1 (*N*-Met-Pro-Arg-Phe-Met-Asp-Try-Trp-Glu-Gly-Leu-Asn-NH_2), while itself soluble in aqueous solution, has numerous hydrophobic residues. Upon conjugation to the thiol linker (Ligand 1), the combination of hydrophobic residues on the peptide and hydrophobic alkane chain of the linker render the ligand water insoluble. Recently, hydrophilic derivative of the p53-based peptide were developed by Zhang et al. (Peptide 2: Phe-Lys-Lys-Ac_6c-Trp-Glu-Glu-Leu).[21] This peptide is designed for cofacial presentation of the key residues (Phe^{19}, Trp^{23}, Leu^{26}) by incorporating features to enhance water solubility and α-helix formation. These include two pairs of Lys (i) and Glu (i + 4) to promote intrahelical electrostatic interactions and the incorporation of the helix promoter 1-amino-1-cyclohexane carboxylic acid (Ac_6c) immediately prior to the Trp residue. To further increase the hydrophilicity of the peptide, and to address the distance between peptide and monolayer, an extra PEG spacer was incorporated between the thiol linker and the N-terminus of the peptide (Figure 1a).

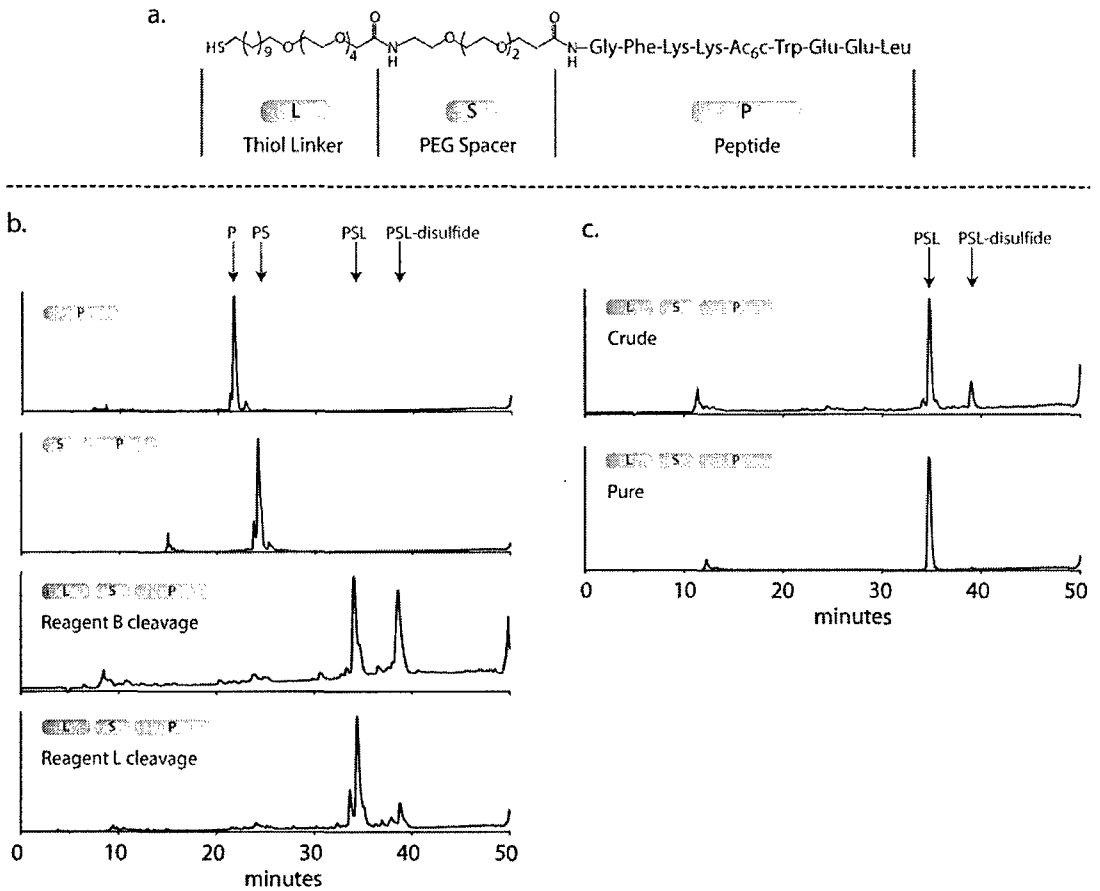

Figure 1: *a. Design of the tripartite Peptide 2 ligand for nanoparticle conjugation, composed of Ligand 1, a novel PEG spacer, and the hydrophilic Peptide 2. b. Analytical HPLC analysis of conjugation product. Resin cleavage/deprotection cocktails lacking*

reducing agents resulted in significant disulfide formation. c. Analysis of final product before and after preparatory HPLC. All HPLC chromatograms represent absorbance at 220 nm.

Peptide 2 was synthesized manually by solid phase peptide synthesis to enable conjugation of the appropriate linker moieties. Standard FMOC chemistry was used to generate Peptide 2. An additional glycine residue was inserted at the N-terminus to increase the spacing between the active peptide segment and the linker moieties. The PEG spacer was designed as an amino acid derivative, facilitating conjugation to the peptide. However, extensive double-coupling using diisopropylcarbodiimide (DIC) was required for complete conjugation. Ligand 1 was conjugated in a similar manner. Each step in the synthesis was monitored by analytical HPLC to ensure completion of the reaction. As seen in Figure 1b, definitive shifts in elution times were observed as each successive moiety was conjugated. Unfortunately, this peptide-linker conjugate was sensitive to oxidation, as significant disulfide formation was observed using a cleavage cocktail lacking a reducing agent, resulting in peptide dimers (as determined by mass spectrometry). Reduction of this disulfide was achieved post-cleavage using tris(2-carboxyethyl)phosphine hydrochloride (TCEP), although reduction was incomplete. This suggests that a certain degree of segregation may take place between the hydrophilic peptide segment and the hydrophobic linker, facilitating the formation of disulfides between closely packed peptide chains. The inefficient reduction of these disulfides by TCEP may be due to the very hydrophobic microenvironment of the disulfide bond, minimized access of the hydrophilic reducing agent. However, a majority of the disulfides can be prevented from forming initially by using a cleavage cocktail containing dithiothreitol (DTT), as demonstrated in Figure 1b. Final purification was achieved using preparative HPLC, resulting in a product that was greater than 90% pure (Figure 1c). Acetylated Peptide 2, lacking the thiol linker and PEG spacer, was also purified to greater than 95% purity. A comparison of inhibitory potential demonstrates that Peptide 2 has a higher IC_{50} than Peptide 1 (0.7 μM vs. 0.3 μM, respectively, see Figure 2).

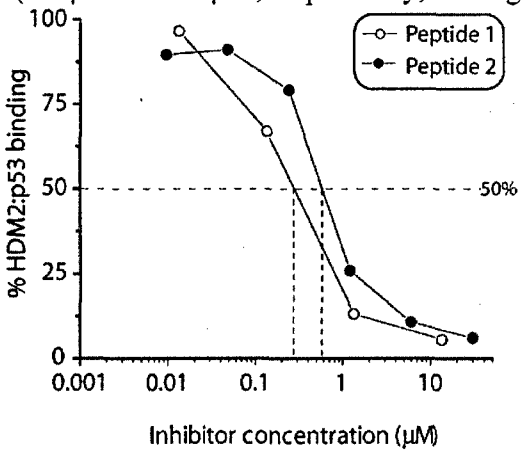

Figure 2. *Comparison of MDM2 inhibition by Peptide 1 and Peptide 2.*

Gold nanoparticles[22] were successfully decorated with the Peptide 2 ligand. Ligand exchange reactions were conducted overnight in water, providing water soluble nanoparticle-peptide conjugates. Nanoparticles could be loaded with varying amounts of peptide, as demonstrated by subsequent electrophoretic mobility shift assays (Figure 3). As each reaction constituent was water soluble, purification was conducted by centrifugation. Due to the small size of

precursor particles (3 nm ± 1 nm), ultracentrifugation at 200,000*g* for 1 hour was required for proper sedimentation. While analysis of the peptide concentrations retained in the wash supernatants afforded approximate quantification of incorporated peptide, residual nanoparticle contaminants in these washes precluded more precise quantification. Due to the polydisperse size range found in the preparation of the nanoparticles, centrifugation may not consistently pellet those particles below 1 nm in size. To address this obstacle, nanoparticles featuring larger gold cores were investigated.

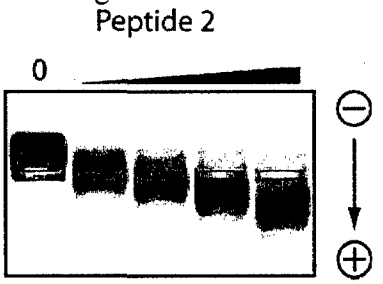

Figure 3. *Electrophoretic mobility of nanoparticles is dependent on the degree of peptide incorporation. Peptide-nanoparticle conjugates migrate to the cathode due to the slight anionic nature of the peptide (pI ≈ 6.5).*

Nanoparticle optimization

To investigate the utility of nanoparticles featuring larger gold cores, citrate-stabilized nanoparticles were synthesized. Citrate-stabilized nanoparticles have been used in recent years for various applications.[23] These particles, due to their larger size, can be easily centrifuged at 13,000 rpm for 30 minutes to form a loose pellet. The synthesis involves the nucleation of gold atoms in the presence of excess sodium citrate. The concentration of citrate dictates the ultimate size of the particle, and citrate functions as a capping ligand on the gold surface. For our application, the synthetic approach of Grabar et al. was used to generate nanoparticles with core diameters of ca.13 nm (NP-1, Figure 4a).[24] Compared to the smaller nanoparticles previously used in this project, the large nanoparticles are significantly more monodisperse in size (Figure 4b).

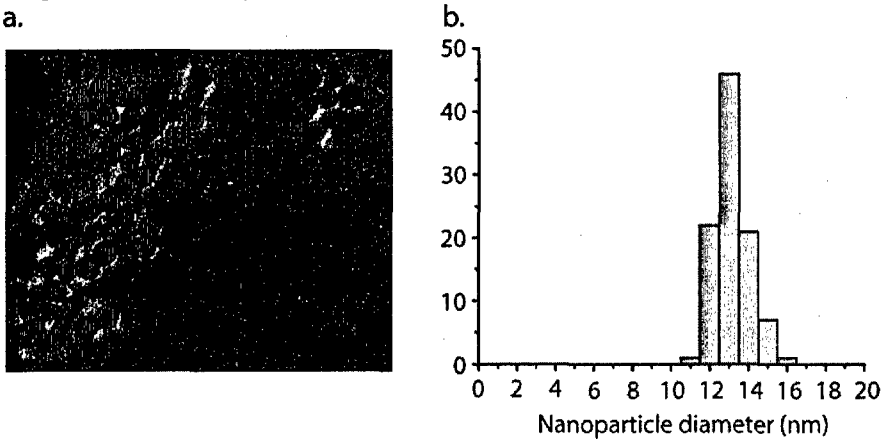

Figure 4. *a. Transmission electron micrograph of citrate-stabilized gold nanoparticle, NP-1. b. Histogram of NP-1 with 13.1 ± 0.9 nm core diameters (error based on S.D.; n = 98).*

Nanoparticles of larger size (core diameters >3nm) have very distinct absorbance profiles, characterized by a surface plasmon band. The position and width of this band can be

correlated to the size and size distribution of the nanoparticle. Also, a shift or broadening of the surface plasmon band indicates a change in core size, perhaps due to particle agglomeration.[25] In the case of 13 nm NP-1, the peak absorbance of this band is at 518, as demonstrated in Figure 5a (black trace). The citrate-stabilized nanoparticles exhibit limited stability in buffered aqueous solutions. This is due to the weak, yet extensive, interactions between the gold surface atoms and citrate. To afford greater stability, as well as biocompatibility, the nanoparticles were exchanged with Ligand 2, featuring the neutral tetra(ethylene glycol) moiety (NP-2). A number of studies have highlighted the difficulty of functionalizing these particles, as displacement of the citrate leads to rapid aggregation of the gold cores. However, the TEG component of Ligand 2 appears to mitigate any interparticle interactions during the exchange, as no agglomeration is observed in the presence of excess ligand. The absorbance spectrum of NP-2 exhibits only a slight shift in the plamson band to 520 nm, without significant broadening (Figure 5a, red trace). The increased stability of NP-2 is demonstrated upon addition of salt (Figure 5b). While NP-1 readily aggregates and precipitates at very low salt concentrations, indicated by a red shift and broadening of the surface plasmon band, the particles functionalized with Ligand 2 are stable even at salt concentrations exceeding 1 M. These nanoparticles can be tailored to incorporate charged functionality on the monolayer periphery, either through subsequent place exchange reactions, or by initial exchange of the NP-1 with mixed ligands (Figure 5c). As seen in Figure 5d, NP-2 (Lane 1) can be completely exchanged with anionic Ligand 1 (lane 2). Mixed monolayers exchanged with 10% Ligand 1 or Ligand 3 can also be achieved (lanes 3 and 4, respectively). These data demonstrate that larger gold core nanoparticles can be readily synthesized and functionalized in an identical manner as our smaller particles.

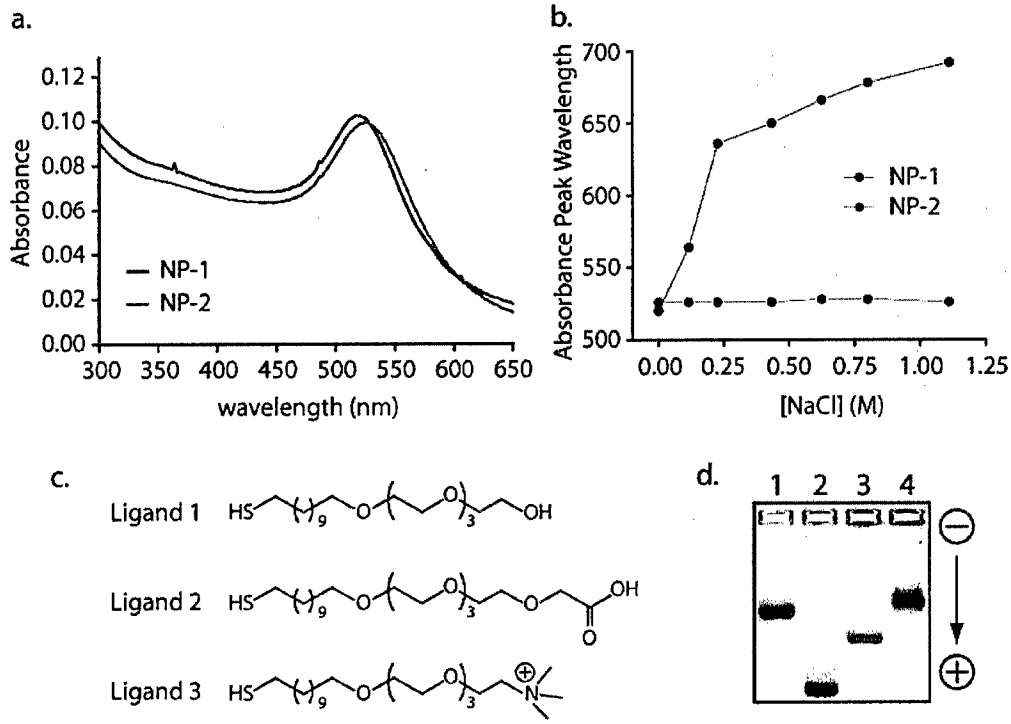

Figure 5. *a. Absorbance spectra of citrate-stabilized nanoparticle before and after exchange with Ligand 2 (black and red traces, respectively). b. Salt-induced shifts in plasmon band are*

observed only with NP-1 not exchanged with Ligand 2. c. Ligands used for place exchange onto NP-2 for charge incorporation. d. Gel electrophoresis of NP-2 derivatives (1, NP-2; 2, NP-2 (100% Ligand 1); 3, NP-2 (10% Ligand 1); 4, NP-2 (10% Ligand 3)).

Nanoparticle-conjugate synthesis and inhibition

Two strategies were used to functionalize citrate-stabilized nanoparticles with Peptide 2 (Figure 6). The first strategy relied on the place exchange of the peptide onto the TEG-functionalized NP-2. Initially, citrate stabilized nanoparticles were exchanged completely with Ligand 2. After purification, the particles were then incubated with the Peptide 2 ligand. Conversely, citrate stabilized nanoparticles were exchanged simultaneously with both Ligand 2 and Peptide 2. Each of these strategies was successful in incorporating peptide into the nanoparticle monolayer, generating NP-3. Gel mobility shift assays indicate that Peptide 2 was successfully incorporated into the NP-2 monolayer (Figure 7a). This is demonstrated by a greater mobility towards the cathode since the peptide is slightly anionic (pI = 6.5). Absorbance spectroscopy corroborates incorporation of Peptide 2, while demonstrating that the ligand exchange reactions have no effect on the nanoparticle core size or size distribution (Figure 7b). Subtraction of the absorbance spectra delineates contribution of the peptide to the NP-3 signal.

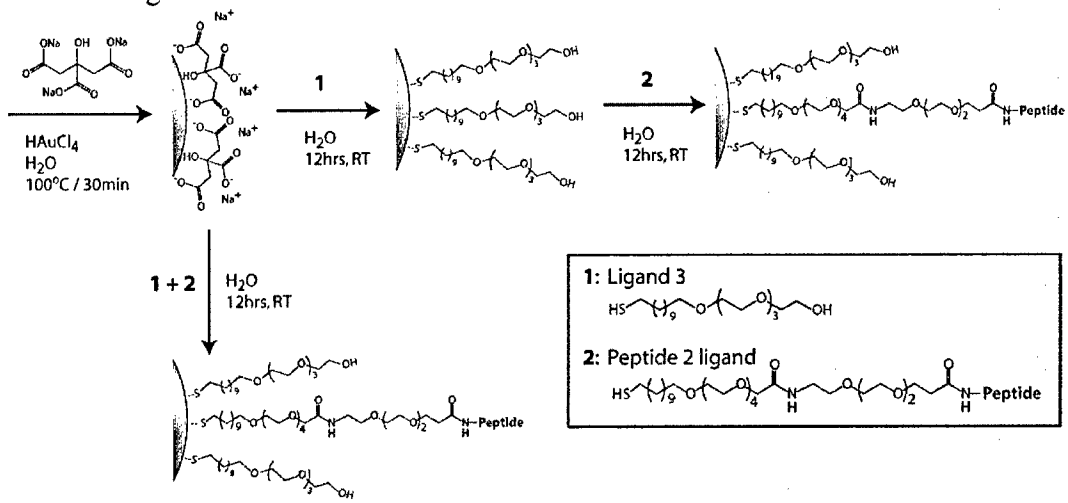

Figure 6. *Incorporation of Peptide 2 ligand into NP-2 monolayer to give NP-3.*

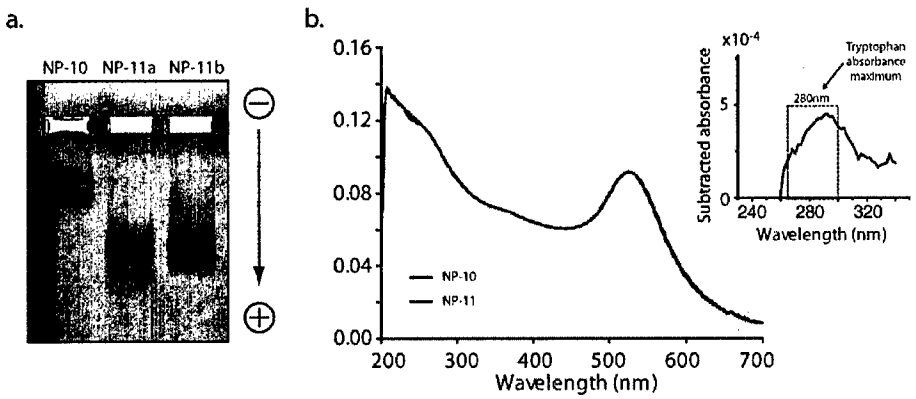

Figure 7. *a. Gel mobility shift of NP-2 and NP3 with two different concentration of incorporated Peptide ligand 2. b. Absorbance spectroscopy of NP-2 and NP-3. Inset of subtracted spectra shows characteristic peptide absorbance at 280 nm.*

To determine the efficacy of NP-3 on inhibiting the p53-MDM2 interaction, an ELISA was performed (Figure 8). Briefly, p53-GST fusion protein was immobilized on glutathione-covered plates. Purified MDM2 was incubated with dilutions of peptide or nanoparticles, followed by subsequence incubation with an anti-MDM2 primary antibody. An alkaline-phosphate-conjugated antibody was the added, and the degree of binding was monitored by the addition of a chromogenic substrate. Unfortunately, the results from the inhibition assay were less striking than found with the previous nanoparticle-peptide conjugate. Inhibition is clearly observed with NP-3b (functionalized with a greater degree of peptide), while little to no inhibition occurs in the presence of NP-2 and N-3a. While disappointing, it is clear that the nanoparticle-peptide conjugates are able to inhibit the p53-MDM2 interaction, albeit with lower efficiency than previously thought.

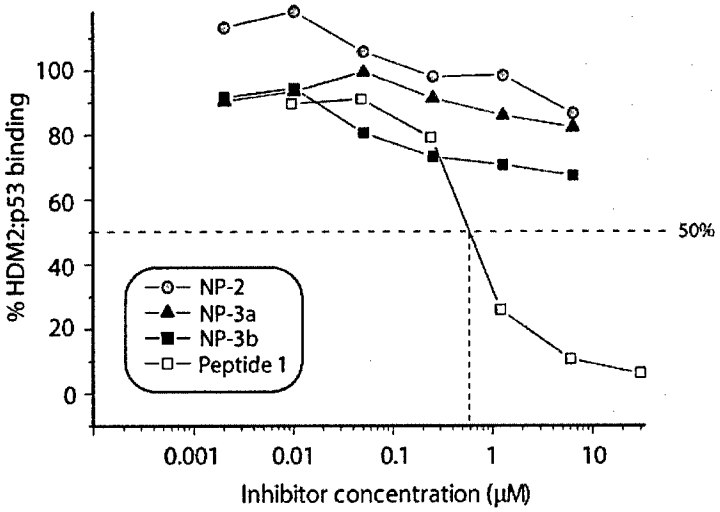

Figure 8. *Inhibition of MDM2 by NP-3.*

Key Research Accomplishments

- Development of hydrophilic peptide
- Optimization of peptide tether, incorporating additional ethylene glycol moieties
- Synthesis of 13 nm gold-core nanoparticles and subsequent functionalization

Training Accomplishments:

This research requires the integration of numerous areas of expertise, from synthetic chemistry to biology. The development of the nanoparticle-based inhibitors allowed me to learn the synthesis of different types of gold-core nanoparticles, including functionalization strategies to enable their use in biological environments. The design of the peptide-based ligand further expanded my knowledge in automated and manual peptide synthesis, chemical

coupling strategies, and the use of analytical and preparatory HPLC. Development and optimization of the ELISA involved molecular cloning, protein expression and purification, and the systematic quantification and analysis of protein binding. Preliminary work in nanoparticle delivery also afforded me the opportunity to work with various cultured cell types and to employ confocal microscopy for live cell imaging. Overall, working on this project has allowed me to greatly expand my technical expertise and, more importantly, to gain insight into the fundamentals of interdisciplinary research.

Reportable Outcomes

Presentations based on project research:

American Chemical Society National Conference (Philadelphia, PA) Aug 2004. *Nanoparticle-mediated rescue of p53 through targeted binding of MDM2.* (Accepted as poster presentation in Division of Organic Chemistry)

Gordon Research Conference: Drug Carriers in Medicine and Biology (Bozeman, MT) Sept 2004. *Nanoparticle-mediated inhibition through protein surface binding.* (Accepted as poster presentation. Could not attend due to medical emergency)

Era of Hope 2005: Department of Defense Breast Cancer Research Program Meeting (Philadephila, PA) June 2005. *Nanoparticle-mediated rescue of p53 through targeted degradation of MDM2.*

Post-doctoral employment offers based on project research:

U.S. Naval Research Laboratory, Division of Optical Sciences (Dr. H. Mattoussi)

Lawrence Livermore National Lab, Chemistry and Materials Science Directorate (Dr. J.B.H. Tok)

Conclusions

The second year of this project began in the hopes of quickly optimizing the nanoparticle and peptide components to facilitate the characterization of the nanoparticle-peptide conjugate. While these goals were accomplished, the outcome fell short of exceptions. The nanoparticles are able to inhibit the p53-MDM2 interaction, but the degree of inhibition is not comparable to free peptide. However, this system can still be optimized for greater efficacy, and the issues will be addressed accordingly.

References

1. D. A. Freedman, L. Wu, A. J. Levine, *Cell Mol Life Sci* **55**, 96-107 (1999).

2. M. Cuny *et al.*, *Cancer Res* **60**, 1077-83 (2000).

3. B. Quesnel, C. Preudhomme, J. Fournier, P. Fenaux, J. P. Peyrat, *Eur J Cancer* **30A**, 982-4 (1994).

4. A. Marchetti *et al.*, *J Pathol* **175**, 31-8 (1995).

5. R. W. Zhang, H. Wang, *Curr Pharm Des* **6**, 393-416 (2000).

6. P. Chene, *Nature Rev. Cancer* **3**, 102 (2003).

7. Garcia-Echeverria, C., Chene, P., Blommers, M. J. & Furet, P. *J. Med. Chem.* 43, 3205–3208 (2000).

8. V. Böttger *et al.*, *Oncogene* **13**, 2141-7 (1996).

9. S. J. Duncan *et al., J. Am. Chem. Soc.* **123**, 554–560 (2001).

10. R. Fasan *et al., Angew. Chem. Intl. Ed.* **43**, 2109-2112 (2004).

11. J. A. Kritzer, J. D. Lear, M. E. Hodsdon, A. Schepartz, *J. Am. Chem. Soc.* **126**, 9468-9 (2004).

12. N. Majeux, M. Scarsi, A. Caflisch, *Proteins* **42**, 256–268 (2001).

13. J. Zhao *et al., Cancer Lett.* **183**, 69–77 (2002).

14. R. Stoll *et al., Biochemistry* **40**, 336–344 (2001).

15. P. S. Galatin, D. J. Abraham, *J. Med. Chem.* **47**, 4163-4165 (2004).

16. L. T. Vassilev *et al, Science* **303**, 844-848 (2004).

17. K. K. Sandhu, C. M. McIntosh, J. M. Simard, S. W. Smith, V. M. Rotello, *Bioconjug. Chem.* **13**, 3-6 (2002).

18. N. O. Fischer, C. M. McIntosh, J. M. Simard, V. M. Rotello, *Proc. Natl. Acad. Sci. U. S. A.* **99**, 5018-23 (2002).

19. N. O. Fischer, A. Verma, C. M. Goodman, J. M. Simard, V. M. Rotello, *J. Am. Chem. Soc.* **125**, 13387-91 (2003).

20. R. Hong, N. O. Fischer, A. Verma, C. M. Goodman, T. Emrick, V. M. Rotello, *J. Am. Chem. Soc.* **126**, 739-43 (2004).

21. R. Zhang *et al. Anal. Biochem.* **331**, 138-46 (2004).

22. A. G. Kanaras, F. S. Kamounah, K. Schaumburg, C. J. Kiely, M. Brust. *Chem. Commun.*, 2294-2295 (2002).

23. N.L. Rosi, C.A. Mirkin. *Chem. Rev.* **105**, 1547-1562 (2005).

24. K.C. Grabar, R.G. Freeman, M.B. Hommer, M.J. Natan. *Anal. Chem.* **67**, 735-743 (1995).

25. C. Burda, X. Chen, R. Narayanan, M.A. El-Sayed. *Chem. Rev.* **105**, 1025-1102 (2005).